ADHD Attention Deficit and Hyperactivity Disorders (2019) 11:91–105
https://doi.org/10.1007/s12402-018-0281-x

ORIGINAL ARTICLE

Effect of disease-associated SLC9A9 mutations on protein–protein interaction networks: implications for molecular mechanisms for ADHD and autism

Yanli Zhang-James[1] · Marc Vaudel[2] · Olav Mjaavatten[3] · Frode S. Berven[3] · Jan Haavik[3,4,5] · Stephen V. Faraone[1,6]

Received: 20 September 2018 / Accepted: 27 November 2018

Abstract

Na^+/H^+ Exchanger 9 (NHE9) is an endosomal membrane protein encoded by the Solute Carrier 9A, member 9 gene (*SLC9A9*). *SLC9A9* has been implicated in attention deficit hyperactivity disorder (ADHD), autism spectrum disorders (ASDs), epilepsy, multiple sclerosis and cancers. To better understand the function of NHE9 and the effects of disease-associated variants on protein–protein interactions, we conducted a quantitative analysis of the NHE9 interactome using co-immunoprecipitation and isobaric labeling-based quantitative mass spectrometry. We identified 100 proteins that interact with NHE9. These proteins were enriched in known functional pathways for NHE9: the endocytosis, protein ubiquitination and phagosome pathways, as well as some novel pathways including oxidative stress, mitochondrial dysfunction, mTOR signaling, cell death and RNA processing pathways. An ADHD-associated mutation (A409P) significantly altered NHE9's interactions with a subset of proteins involved in caveolae-mediated endocytosis and MAP2K2-mediated downstream signaling. An ASD nonsense mutation in *SLC9A9*, R423X, produced no-detectable amount of NHE9, suggesting the overall loss of NHE9 functional networks. In addition, seven of the NHE9 interactors are products of known autism candidate genes (Simons Foundation Autism Research Initiative, SFARI Gene) and 90% of the NHE9 interactome overlap with SFARI protein interaction network PIN ($p < 0.0001$), supporting the role of NHE9 interactome in ASDs molecular mechanisms. Our results provide a detailed understanding of the functions of protein NHE9 and its disrupted interactions, possibly underlying ADHD and ASDs. Furthermore, our methodological framework proved useful for functional characterization of disease-associated genetic variants and suggestion of druggable targets.

Keywords ASDs · ADHD · *SLC9A9*/NHE9 · Protein–protein interaction · Network · Mass spectrometry · Endocytosis · Drug targets

Introduction

Genome-wide association studies (GWAS) show that hundreds or possibly thousands of common and rare genetic variants contribute to the risk for attention deficit hyperactivity disorder (ADHD) and autism spectrum disorders

This manuscript is in response to a special issue honoring Prof. Jan Buitelaar.

Electronic supplementary material The online version of this article (https://doi.org/10.1007/s12402-018-0281-x) contains supplementary material, which is available to authorized users.

✉ Stephen V. Faraone
sfaraone@childpsychresearch.org

[1] Departments of Psychiatry, SUNY Upstate Medical University, 750 East Adams St., Syracuse, NY 13210, USA

[2] Department of Clinical Science, University of Bergen, Bergen, Norway

[3] Department of Biomedicine, University of Bergen, Bergen, Norway

[4] K.G. Jebsen Centre for Research on Neuropsychiatric Disorders, University of Bergen, Bergen, Norway

[5] Division of Psychiatry, Haukeland University Hospital, Bergen, Norway

[6] Neuroscience and Physiology, SUNY Upstate Medical University, 750 East Adams St., Syracuse, NY 13210, USA

(ASDs) (Lee et al. 2013; Faraone and Mick 2010). Both disorders are highly heritable and share many common and rare genetic risks (Hultman et al. 2007; Zafeiriou et al. 2013; Antshel et al. 2013; Williams et al. 2012). One such shared risk gene is *SLC9A9*. *SLC9A9* was first implicated in ADHD by a report of an extended family in which ADHD co-segregated with a pericentric inversion of chromosome 3 which disrupted the gene (de Silva et al. 2003). Several association studies of ADHD reported significant findings in *SLC9A9* (Brookes et al. 2006; Lasky-Su et al. 2008b; Markunas et al. 2010; Zayats et al. 2015; Demontis et al. 2017). A homozygous deletion near the 5′ transcription initiation region of *SLC9A9* was found in a patient with both autism and epilepsy (Morrow et al. 2008), and several other rare mutations in *SLC9A9* have been reported (Kondapalli et al. 2013; Wagle and Holder 2014). *SLC9A9* was also found nominally associated with nicotine dependence (Uhl et al. 2007), which is also associated with ADHD (Biederman et al. 2009; Monuteaux et al. 2007). In addition, *SLC9A9* was found associated with multiple sclerosis (MS) disease activity (Liu et al. 2017; Esposito et al. 2015) and several forms of cancers (Ng et al. 2008; Chen et al. 2015; Esposito et al. 2018).

SLC9A9 protein (NHE9) localizes on the membranes of late recycling endosomes (Nakamura et al. 2005), critical cellular component for recycling and degradation of neurotransmitter receptors and transporters (Melikian and Buckley 1999; Park et al. 2004; Hirling 2009; Martin-Negrier et al. 2006; Daniels and Amara 1999). This pathway is implicated in synaptic long-term potentiation (Park et al. 2004, 2006), which underlies learning and memory, cognitive functions frequently disrupted in ADHD and ASDs (Sowerby et al. 2011; Martinussen and Tannock 2006; Solomon et al. 2015; Patak et al. 2016). The *Slc9a9* knockout mouse exhibits ASD-like behavioral deficits (Yang et al. 2016; Ullman et al. 2018) and rats with *Slc9a9* mutations showed inattentive ADHD and ASD-related phenotypes (Zhang-James et al. 2011, 2014; Sagvolden et al. 2008). However, the NHE9 interactome is not well characterized. Two proteins, calcineurin homologous protein (CHP) (Zhang-James et al. 2011) and receptor for activated C-kinase 1 (RACK1) (Ohgaki et al. 2008; Zhang-James et al. 2011), were reported to bind to NHE9 C-terminal in co-IP and western blot experiments. Additional two proteins, tumor protein P53 (Daakour et al. 2016) and zinc finger, DHHC-type containing 17 (Butland et al. 2014) were found to bind to NHE9 in yeast-two-hybrid screenings. The *Slc9a9* mutations in the inattentive ADHD rats were found to increase the interactions with CHP (Zhang-James et al. 2011), and potentially resulted in a host of coordinated gene expression changes involving the predicted binding partners and their downstream targets in these animals (Zhang-James et al. 2012). These observations suggested that disease-relevant variants in *SLC9A9* could alter the functional protein networks that are relevant to the disease pathophysiology.

Indeed, studies of complex multifactorial genetic disorders often find that risk variants tend to converge on protein network clusters and functional pathways. Exome sequencing studies of ASDs show that genes with rare single-nucleotide variants (SNVs) encode proteins that are significantly enriched in specific protein–protein interaction (PPI) networks relevant to brain function (Neale et al. 2012; Sanders et al. 2012; O'Roak et al. 2011, 2012). Other work shows substantial overlap in the neuronal networks implicated by rare SNVs, rare copy number variations (CNVs) and common DNA variants for ASDs (Ben-David and Shifman 2012). The genes implicated in ASDs by rare variants are in the same pathways as known genes implicated by syndromic ASDs, particularly those involved in synaptic functions (Sakai et al. 2011); studies of the ASD transcriptome have drawn the same conclusion (Lanz et al. 2013). GWAS of ADHD presented enrichment of genes from similar neurodevelopmental pathways as of ASDs, such as those involved in synaptic development and functioning (Poelmans et al. 2011; Yang et al. 2013). In the past, a number of proteomic studies in ASDs were published in an attempt to identify proteomic biomarkers (Ngounou Wetie et al. 2014; Woods et al. 2013; Ngounou Wetie et al. 2015). In particular, one study has examined the impact of alternative splicing isoforms on PPI networks for ASDs genes using yeast-two-hybrid method (Corominas et al. 2014). Proteomic studies of ADHD are more limited (Pivac et al. 2011; Taurines et al. 2010). However, to the best of our knowledge, no study has examined how the disease-associated variants alter the protein–protein interactions in a high-throughput quantitative fashion.

Here, we extend our prior work of SLC9A9 by using co-immunoprecipitation (Co-IP) and mass spectrometry to assess the impact of protein coding mutations on NHE9's PPI network. We set out to investigate two known human disease-associated mutations in this study: (1) a nonsense mutation (R423X), found in an autistic patient with epilepsy (Morrow et al. 2008); and (2) a non-synonymous mutation (A409P) found in an ADHD patient with obesity in a genome-wide association study sample (Lasky-Su et al. 2008a, b). Our overarching hypothesis is that rare single-nucleotide variants in SLC9A9 increase the risk for ADHD and ASDs by disrupting PPI networks. By describing these PPI networks and examining the effects of functional variants, we expected to gain insight into the molecular pathophysiology of these disorders. Furthermore, investigation of mutant-induced alterations in the PPI network can suggest targets for drug discovery.

Experimental procedures

Cloning, transfection and Co-IP

Rat SLC9A9 coding sequence (NM_001271438) with stop codon was amplified by PCR and cloned into a mammalian expression vector (pDsRed1-N1) with an N-terminal C-Myc-tag as described previously (Zhang-James et al. 2011). Mutations were made by site-directed mutagenesis. Two constructs for the R423X mutation were created. One had a single-point mutation in the full-length cDNA to replace the 423aa with a stop codon. The other contains a truncated cDNA (TRK) for the first 422 amino acids. 48 h post-transfection using Lipofectamine®2000 reagents (Life Technologies, Grand Island, NY), HEK293 cells were lysed in phosphate-buffered saline (PBS) buffer supplemented with 1% Lauryl-β-D-maltoside (DDM) and 1 × Halt protease and phosphatase inhibitor cocktails (Piercenet, Rockford, IL). Expression of tagged NHE9 protein was verified by western blot (WB) using both anti-Myc (Abcam, Cambridge, MA) and anti-NHE9 antibodies (ProteinTech, Rosemont, IL). Empty vectors were transfected in negative control groups (CT).

Experimental design for Co-IP and tandem mass tag (TMT)-labeled MS samples

5 mg of cell lysate was used for each co-IP with 15 µl Anti-c-Myc Agarose (Piercenet, Rockford, IL) overnight at 4 °C, followed by four gentle washes using PBS with 0.1% DDM. Proteins were eluted with 50 µl 2 × Lane Marker reducing sample buffer (Piercenet, Rockford, IL). 2 µl was used for western blot to verify the pull down of c-Myc-tagged NHE9, and 48 µl was stored at − 20 °C until use. CT lysates served as no-bait negative controls. Two independently processed and verified eluates were combined as one co-IP sample (96 µl total) to provide ~ 20 µg total proteins/sample for TMT labeling. A total of 15 co-IP samples were produced and were partitioned into four TMT-labeled MS samples according to Supplementary Figure 1A. Three pairs of wild type (WT) versus CT co-IP samples were labeled with 6-plex TMT reagents and grouped as one sample for MS acquisition. Three additional MS samples were each composed of one set of three parallel-processed IP samples: WT, A409P (AP) mutant and CT. These samples were also labeled with 6-plex TMT reagents with a balanced design.

TMT labeling and MS acquisition

Co-IP samples were first precipitated with 6 × volumes of cold acetone at − 20 °C overnight and fully re-suspended in 4.2 µl of 10 M urea. Urea was gradually diluted with dissolution buffer, reducing agent tris-(2-carboxyethyl) phosphine (TCEP) and alkylating agent iodoacetamide (IAM) to a final concentration of 4.9 M prior to a 6 h predigestion with 200 ng recombinant Lys-C (Promega) at 37 °C. Samples were then added with 0.7 µl denaturant (2% SDS) and diluted with dissolution buffer to obtain 1.5 M urea concentration for an overnight digestion with 2 µg trypsin. Dissolution buffer was then removed in a SpeedVac concentrator, and dried peptide pellets were shipped to the Proteomics Unit at the University of Bergen (PROBE, Bergen, Norway) for TMT labeling and MS/MS acquisition. TMT 6-plex™ reagents were used to label the digested peptides following manufacturing protocols (Piercenet, Rockford, IL) according a balanced design in the Supplementary Figure 1A (Mahoney et al. 2011). After pooling, the resulting four MS samples were subsequently cleaned using Cation Exchange cartridges and desalted using a reversed phase Oasis® HLB Elution plate (2 mg sorbent per well, 30 µm particle size; Waters Assoc, MA) before LC–MS/MS analysis using an Ultimate 3000 RSLCnano system in line with an LTQ Orbitrap ELITE (Thermo Fisher Scientific).

LC–MS/MS analyses were conducted as described previously (Aasebo et al. 2014; Guldbrandsen et al. 2014) with minor modifications (Supplementary File 1). The full-scan MS and MS/MS spectra were searched against reviewed human protein sequences (Uniprot, downloaded April 2013) using the SequestHT search engine implemented in Proteome Discoverer 1.4 (Thermo Fisher Scientific). The search settings are described in Supplementary file 1. Only master proteins from each group were considered for the statistical analysis. Calculations of fold change were performed on Extracted Ion Chromatograms (XIC) of the reporter ions corrected for isotopic impurities. Reported TMT ratios include each bait protein IP channel (WT and Mut) versus the CT channel as well as the Mut versus WT ratios (Supplementary Figure 1A, B).

Statistical analysis for PPI filtering

TMT ratios (WT vs CT or AP vs CT) were calculated for each MS acquisition. We followed the general statistical recommendations for data normalization and statistical analysis by Oberg and Mahoney (2012) and Oberg and Vitek (2009). First, the TMT ratios were log2 transformed and quantile normalized. We then used the "removeBatchEffect" function from LIMMA (version 3.26.9), an R(version 3.2.4)/Bioconductor package, to remove batch effect between MS runs (Smyth and Speed 2003; Ritchie et al. 2015). Results were further standardized and subjected to a *Z* test for PPI filtering. Raw TMT ratios, log2 transformed and normalized ratios are plotted in Supplementary Figure 1B. The main hypothesis for PPI filtering is: if a protein is present

in higher abundance in the IP sample than the CT sample, then it is likely due to a real interaction with the bait protein; non-specific pull down would result in a similar (or lower) yield for the IP samples than for CT. Therefore, we used a one-tailed *Z* test to determine if a protein has a log IP versus CT ratio above 0 (Fig. 1a, b).

The AP versus WT ratios were also normalized and scaled using the same methods. We used a two-tailed *Z* test to determine if a protein has a log AP versus WT ratio that is statistically significantly different from 0, which suggests that protein is precipitated in different amount with the mutant bait from that with the WT bait (Fig. 1c). We define these proteins as interactors with either increased or decreased interactions with NHE9 due to the mutation.

For both sets of analysis described above, only proteins identified in two or more MS samples were subjected to the *Z* tests. An alpha level of 0.05 was used with Bonferroni correction based on total numbers of available comparisons for each test.

Network pathways and functional analysis

Ingenuity Pathway Analysis software (IPA®, QIAGEN, Redwood City, CA) identified the canonical pathways implicated by the WT and AP PPIs, as well as the AP-changed PPIs. IPA uses Fisher's Exact Test with Benjamini–Hochberg correction to determine whether a pathway is enriched within a list. We compared our PPI networks with the ASD PPI network curated by SFARI (https://gene.sfari.org/autdb/PINHome.do) and tested for overlap using Fisher's Exact Test. To ensure that our overlapping analyses were not capitalizing on chance variation, we used IPA's database to derive PPI networks implicated by other ASD risk genes and then again for non-ASD genes, derived from bone mineral density (BMD) studies (Ralston and de Crombrugghe 2006), as a negative control. These protein networks were compared with our NHE9 PPIs for their overlap with the SFARI network. We also used IPA to retrieve drugs targeting the PPIs. These were based on drug-target relationships from the Ingenuity Knowledge Base curated from multiple sources.

Network topology analysis

We used IPA protein–protein interaction databases to construct the known relationship between the identified proteins. The resulted IPA PPI networks were then imported to Cytoscape (v3.2.1) (Shannon et al. 2003) for visualization and topology analysis using the Cytoscape Network Analyzer plugin (Assenov et al. 2008).

PPI validation

We verified NHE9 and two binding partners in the Co-IP products by western blot (WB). Antibodies used were:

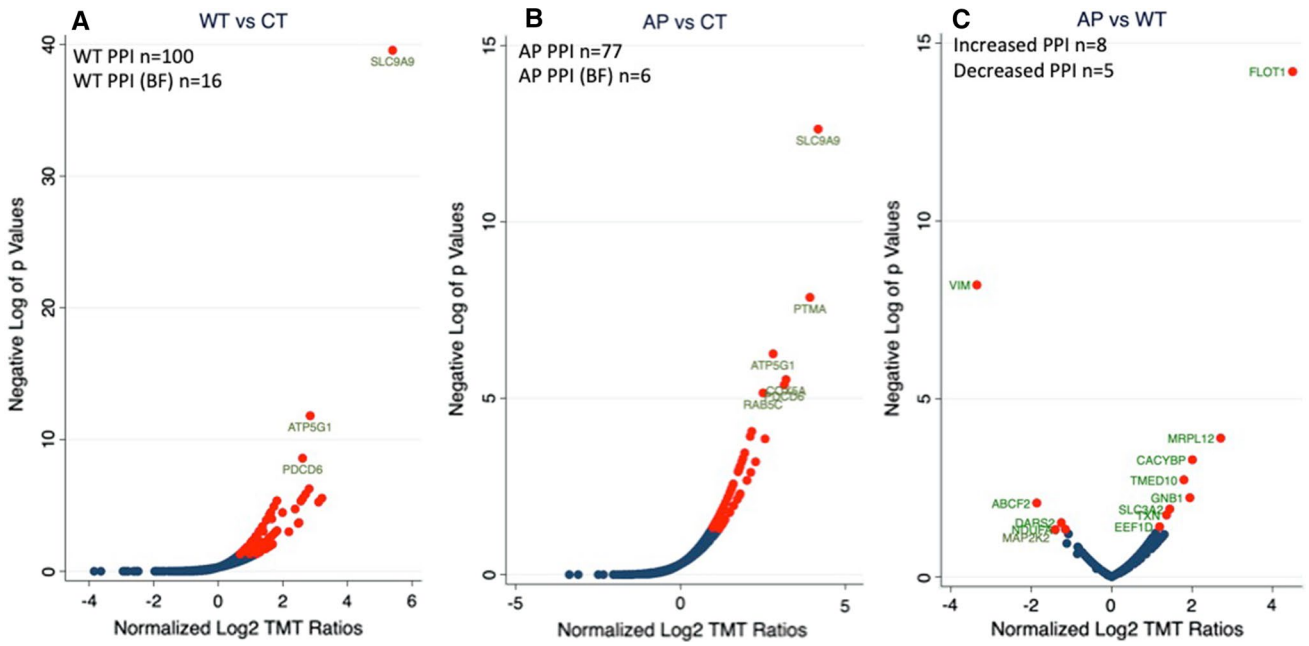

Fig. 1 PPI filtering using a one-sided *Z* test for WT PPIs (**a**) and AP PPIs (**b**) and a two-sided *Z* test for AP induced changes (**c**). Results were plotted as negative log *p* values (*y*) versus the averaged normalized log ratios (*x*), which are the ratios of WT versus control (CT) IP (**a**), the ratios of AP versus CT (**b**) and the ratios of AP versus WT (**c**). Proteins highlighted in red were those met *Z* test $p < 0.05$, and names were labeled for the top findings. We also notate the total number of PPI that met *Z* test $p < 0.05$, as well as those were remained significant after Bonferroni corrections (BF)

NHE9 (ProteinTech, Chicago IL), transferrin receptor (TFRC) and HRP-conjugated c-Myc (Myc-HRP) antibodies from Abcam (Cambridge, MA), RACK1 antibodies from Novus Biologicals (Littleton, CO), MAP2K2 from Thermo Scientific (Waltham, MA). RACK1 was one of previously known NHE9 PPIs. MAP2K2 was chosen because it was one of the AP altered PPIs and because of its interesting role in the MAPK signaling pathways and its relationship with the autism genes EIF4E. TFRC was chosen for its role in endosomes. Bands were visualized using chemiluminescent substrate and imaged in BioRad ChemiDoc MP system (Hercules, CA). Each protein was verified in at least two independent co-IP experiments. Band intensities were measured using ImagJ (Schneider et al. 2012) and subtracted from the background and normalized to the ratios to that of the CT lanes. Differences in band intensities were evaluated by Fisher's PLSD post hoc test following ANOVA.

Endocytosis assays

Endocytosis pathways were examined in Neuro-2a (N2a) cells transfected with WT or A409P mutant SLC9A9 using FITC-conjugated transferrin (TF) and Alexa Fluor 488-conjugated Cholera Toxin Subunit B (CTB, Thermo Fisher). TF binds to TF receptors and is internalized via the clathrin-medicated endocytosis pathway (Mayle et al. 2012). CTB binds to membrane ganglioside GM1 within the lipid rafts and can be internalized mainly via the caveolae-mediated pathways, and also the clathrin-mediated, and clathrin-/caveolae-independent endocytosis pathways (Chinnapen et al. 2007). Transfected N2a cells were plated at 2×10^5 cells/well in 24 well plates for overnight adherence prior to the labeling. Labeling is initiated by incubating cells in serum-free DMEM medium (Thermo Fisher) for 1 h and followed by incubation with 50 µg/ml TF or 2 µg/ml CTB for 10, 30 or 60 min at 37 °C. Non-labeled cells were incubated with only serum-free medium (0 min labeling). Non-internalized ligands were removed by two changes of cold acid wash (0.2 M acetic acid, 0.2 M NaCl in PBS), and two PBS rinses. Cells were then fixed with 4% paraformaldehyde in PBS, stained with 4′,6-diamidino-2-phenylindole (DAPI) for nuclei and imaged in an inverted fluorescence microscope. Two replicates wells were labeled for each transfection group and each time point. Eight full-field images were obtained for each replicate using a grid-guided systematic random sampling technique. Each field was imaged with both a GFP filter for the internalized ligands and a DAPI filter for nuclei. All fields were imaged using a 10× objective with the same optimized settings, including the cells that were not labeled with TF or CTB, the intensity of which was used as background and was subtracted from those with the internalized ligands. Fluorescence intensities were measured following a "rolling ball" algorithm using the batch-processing function in ImageJ software (Schneider et al. 2012). We calculated the endocytosis index for each image as the ratio of the corrected TF or CTB intensities vs those of the DAPI intensity, with the denominator used to correct for different cell densities. Differences between transfection groups were evaluated by Fisher's PLSD post hoc test following ANOVA.

Results

Bait protein expression, Co-IP verification and MS protein identification

The WT and mutant A409P proteins were expressed equally abundantly in 48 h post-transfected cells and migrated to approximately 70 and > 150 kDa on the SDS-PAGE gel (Fig. 2). Although both bands contain multiple species of proteins, likely from various post-translational modifications of monomers, dimers and aggregates, they were verified by both anti-Myc-tag and anti-NHE9 antibodies (Figs. 2, 4) (Zhang-James et al. 2011). Modified and dimerized are functional forms for NHEs (Hisamitsu et al. 2006; Malo and Fliegel 2006). Detergent-resistant aggregates of high

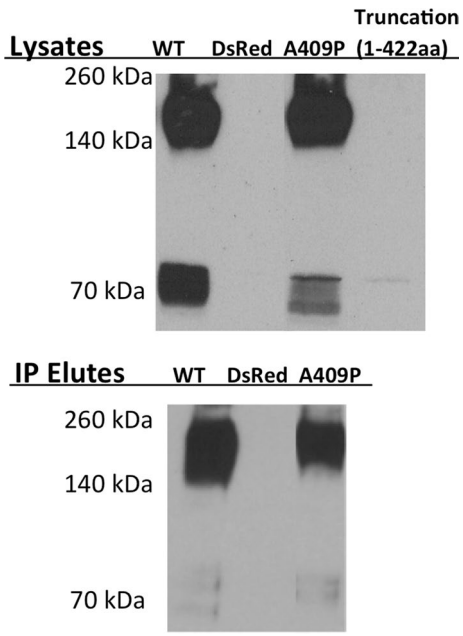

Fig. 2 Western blot verification of NHE9 expression and IP products. Top. WT and A409P constructs were expressed as both monomers and dimers in the cell lysates; whereas the R423X mutant (not shown) and a truncated (1-422aa) construct were not detected. Bottom IP elutes detected a similar yield of bait proteins with more dimers than monomers for WT and both mutants. These bands were detected using anti-Myc-tag antibody, but also confirmed using an anti-SLC9A9 antibody later (see Fig. 4). WT = wild type NHE9 bait protein. DsRed is the empty vector used in the negative control samples

molecular weight are often observed in SDS-PAGE gels for NHE proteins due to their propensity to form strong hydrophobic interactions (Bullis et al. 2002). In our IP eluates, a majority of NHE9 are higher molecular weight products, suggesting that the IP procedure may have promoted dimerized and aggregated forms. The full-length cDNA with R423X mutation failed to produce detectable protein by antibodies (not shown). A truncated version (1-422aa) was not detectable by western blot either. Thus, the R423X mutation was not included in subsequent studies.

From the four MS samples consisting of 15 TMT-labeled co-IP samples (Supplementary Figure 1A), 1483 proteins met protein identification criteria (listed in Supplementary file 2). Among them, 288 proteins were identified from all four MS samples and 539 proteins were identified in two or three samples.

Statistical filter of PPIs

Z tests of standardized and normalized log2 TMT ratios of IP versus CTs identified 100 proteins significantly precipitated with WT NHE9 proteins and 77 with the AP mutant. These are highlighted in red in Fig. 1a, b where the negative log *p* values are plotted against the mean IP versus CT ratios. We confirmed that bait protein NHE9 was the most abundant protein in the IP samples. It had the highest IP versus CT ratios and the most significant *p* values. Fifty proteins were in common for WT and AP NHE9. Among the total of 127 proteins that are either WT or AP interactors, 8 showed significantly increased precipitation and 5 showed significantly decreased precipitation due to the AP mutation (Fig. 1c). Supplementary File 2 lists the *Z* test results for all proteins. Supplementary Figure 2 plots the distribution of percentage of protein coverage, the numbers of Peptide Spectrum Matches (PSMs) and peptides identified for each protein against the normalized mean WT versus CT ratios and the *Z* test negative log *p* values, showing that these factors do not influence the *Z* test-based PPI filtering.

Functional analysis of the PPIs

PPI lists were imported into IPA for functional pathway analysis. Supplementary File 3 lists the negative log *p* values for the top canonical pathways. A number of known endosome-related pathways were significantly enriched for WT or AP PPIs: the clathrin- and caveolae-dependent endocytosis signaling, phagosome maturation, unfolded protein response and protein ubiquitination pathways. Several of the most enriched pathways, such as mitochondrial dysfunction, oxidative phosphorylation, apoptosis and cell adhesion, had not previously been associated with NHE9. IPA's drug-target database listed eight WT or AP PPIs as druggable targets (MAP2K2, XPO1, TXN, PRKDC, CA2, SLC25A5, SLC25A6, PKM). MAP2K2, a PPI that is significantly decreased by the AP mutant, and TXN, an AP increased PPI, are targets of several FDA-approved anti-cancer drugs.

The SFARI Gene Base curates all known genes implicated in ASD and provides a comprehensive protein interaction network (PIN) derived from all known/published interactions with the products of these genes. Among the 100 WT PPIs, seven were coded by SFARI ASD candidate genes: ACTN4, EIF4E, ETFB, PRKDC, RBM27, RHEB and XPO1. RHEB and EIF4E were also AP PPIs. Furthermore, 90% of both the WT and AP PPIs overlap with the SFARI PIN (Fisher's exact test $p < 0.0001$). To assess if these significant findings were spurious, we took a two-stage approach. First, we determined if a similar analysis would show a significant overlap of known ASD candidate genes with the SFARI network, which would be expected. To test this hypothesis, we examined four known ASDs genes, *FMR1*, *CACNA1C*, *MECP2* and *SHANK3.* Second, we expected that the SFARI network would not show significant overlap with PPI networks derived from six proteins implicated in bone mineral density (BMD):*SOST*, *OPG/TNFSF11, PPARG, IGF1, ALOX12* and *AR* (Ralston and de Crombrugghe 2006). For each gene, we generated a PPI network from proteins extracted from IPA's database. Each PPI network (one derived from each gene) was examined for overlap with the SFARI PPI network. Figure 3 shows that the networks derived from autism candidate genes have a highly significant overlap with the SFARI network, similar to what we found for NHE9's PPI network. In contrast, the BMD PPI networks had a lower and nonsignificant overlap with the SFARI network. The only exception was for the BMD gene, androgen receptor (*AR*), which is also a SFARI ASD candidate gene (Henningsson et al. 2009).

Network topology results

Based on the IPA PPI database, 71 WT proteins were connected by known interactions to form a single clustered network (Supplementary Figure 3A). The majority of the remaining proteins were singletons that were not known to connect with any other proteins in the NHE9 PPI network. Since the proteins in the NHE9 network are all precipitated with NHE9, we hypothesize that the singletons bind to NHE9 directly, while proteins in the main cluster may have indirect interactions with NHE9 via macromolecular complexes. AP proteins also formed a single cluster. Only 47 AP proteins were connected (Supplementary Figure 3B).

Following network naming convention, we refer here to the proteins in the network as nodes and the interactions as edges. Network topology analysis of the WT and AP connected networks showed that both main clusters of the networks have a diameter of 7 (the maximal shortest path between two nodes, corresponding to the maximum

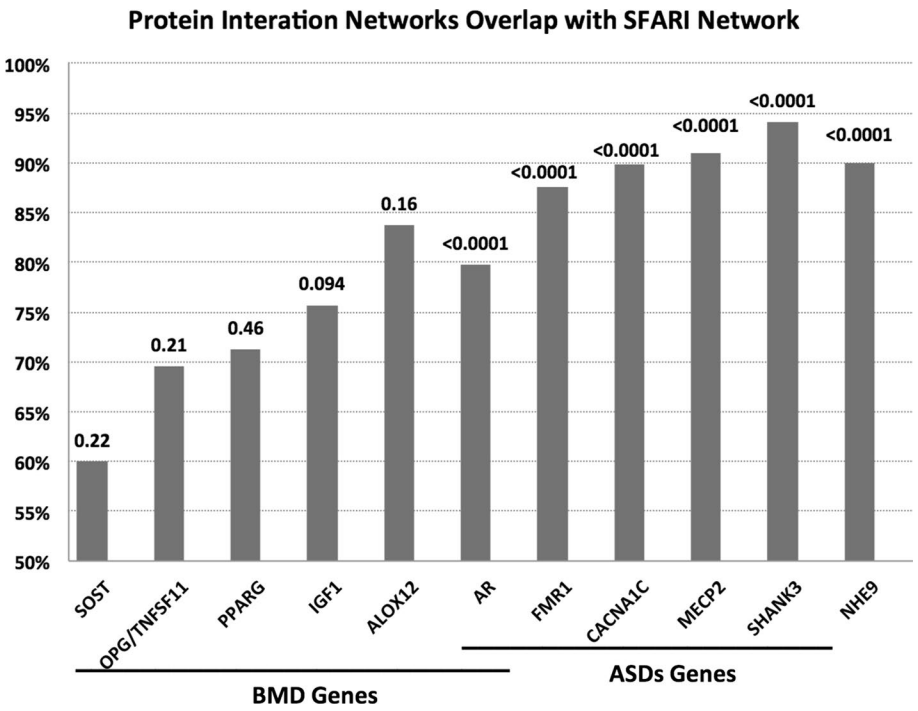

Fig. 3 The degree of overlap of protein interaction networks with the SFARI ASD gene PPI network. The PPI networks derived from IPA database for each gene on the horizontal axis are compared with the SFARI ASD PPI network. The percentages of proteins that overlap with the SFARI network are plotted as bars, and the overlap p values are labeled for each gene. Six BMD genes, derived from a review of genetic regulation of bone mineral density and four well-known ASDs genes, are examined in comparison with the NHE9 WT PPI network. Note that one BMD risk gene, AR, is also a SFARI ASD candidate gene. Fisher's exact test p values are used to evaluate the degree of overlap. All the ASDs genes are highly significant ($p < 0.0001$). None of the BMD genes, except AR, are significant

eccentricity of the nodes) and a radius of 4 (minimum of the nonzero eccentricity of the nodes). Topologically, both networks have the typical characteristics of most biological networks, which consist of a few hubs of high degree and a majority of nodes that only connect to a few hub nodes.

In contrast to the above similarities shared between the WT and AP network, the WT network had a substantially higher clustering coefficient (0.255) than the AP network (0.091). The network clustering coefficient is the average of clustering coefficients of all nodes (from 0 to 1), which measures the ratio of total connections between the neighbors to the maximum possible such links. Therefore, this finding suggests that nodes in the AP network are less connected compared to the WT network. Indeed, on average the nodes in WT network had 3.92 neighbors and nodes in AP network had 3.06 neighbors. We graphed the WT and AP networks in Supplementary Figure 3, with the size of the nodes corresponding to their degrees (numbers of connected neighbors) and the color highlighting those significantly changed by the A409P mutation (Z test $p < 0.05$). Note that VIM, one of the most connected nodes (degree of 8), was the most significantly decreased PPI. The loss of VIM and its neighbors in the AP network may account for the reduced connectivity within the network. Other notable changes are the loss of MAP2K2 and acquired interactions with FLOT1 and other proteins.

Western blot (WB) validation

Western blots verification of bait protein NHE9 and two targets TFRC and MAP2K2 all showed that bands in WT co-IP lanes were stronger than those in the CT lanes (Fig. 4a, b), confirming the validity of our quantitative mass spectrometry methods in identifying PPIs. TFRC had both ~90 kDa (monomer) and ~180 kDa (dimer) bands in the Co-IP lanes (Turkewitz et al. 1988), which were both almost absent in the CT lane (Fig. 4b). Consistent with the MS results, WB confirmed that MAP2K2 was pulled down with WT NHE9 (compared with CT, $p = 0.02$) and that it was markedly reduced in the AP eluates. However, the difference between WT and AP for WB results was not statistically significant (Fig. 4e). We also verified one of previous known interactors, RACK1. Figure 4d showed that RACK1 was present in both WT and AP eluates. However, RACK1 was also present abundantly in the CT eluates, although at lower level, suggesting that our IP procedures did not remove all non-specific bindings.

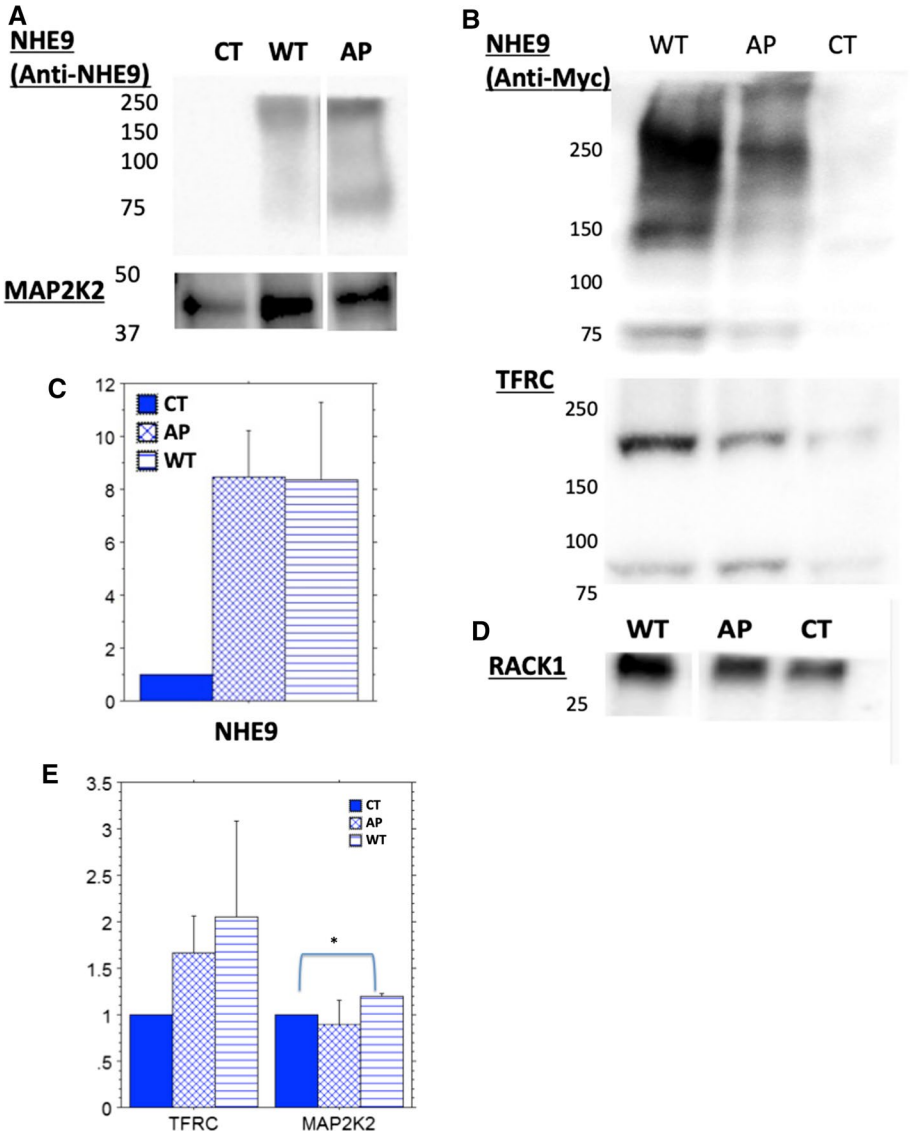

Fig. 4 Western blot verification of bait (NHE9) and selected binding partners. CT, no-bait control IP; WT, WT NHE9; AP, the A409P mutation. **a** Top WB confirmed the successful pull down of the bait NHE9 using anti-SLC9A9 antibody and the bottom portion showed the co-precipitation of MAP2K2 preferentially in the WT IP lane. **b**. Top portion showed another IP verification of NHE9 with the anti-SLC9A9 antibody, and the co-precipitation of TFRC in the same prep. **c** Band intensity quantification was shown for NHE9. **d** Verification of co-precipitated RACK1 protein in the IP elute. **e** Quantification of MAP2K2 and TFRC. For both C and E quantifications, band intensities were subtracted from the background and normalized to the ratios to that of the CT lanes. In E, star (*) indicates the significant difference between WT and CT intensities ($p < 0.05$). The difference was lost in AP lane

Functional validation

Transferrin (TF) and CTB underwent rapid endocytosis in N2a cells. The fluorescent ligands were readily observed in endosomes as punctuated patches at 10 min. Supplementary Figure 4A shows the uniform labeling pattern for TF. But CTB endocytosis appeared to be more heterogeneous among cells. Representative images for each time point are shown in Supplementary Figure 4B, C. Quantification (Fig. 5) showed that both WT and A409P transfected N2a cells demonstrated greater TF endocytosis than non-transfected and empty-vector transfected control groups. This effect peaked at 30 min (group effect $F_{(3,60)} = 7.84$, $p = 0.0002$). On the contrary, CTB endocytosis was reduced in WT and A409P transfected groups similarly at 10 and 30 min. However, A409P cells showed persistently lower CTB intensity at 60 min, while WT-transfected cells were similar to the empty-vector transfected groups. The difference between A409P and WT groups was significant at 60 min ($t = 2.29$, $p = 0.026$).

Discussion

GWAS and sequencing studies are providing an increasing number of disease-associated variants. One step toward understanding how these variants lead to disease etiology is through understanding how they affect functional protein networks. Our study is one of the first to use quantitative MS with Co-IP to study PPI networks for disease-associated genetic variants. We identified ~ 100 proteins that directly or indirectly interact with NHE9, some of which were significantly changed by disease-associated mutation.

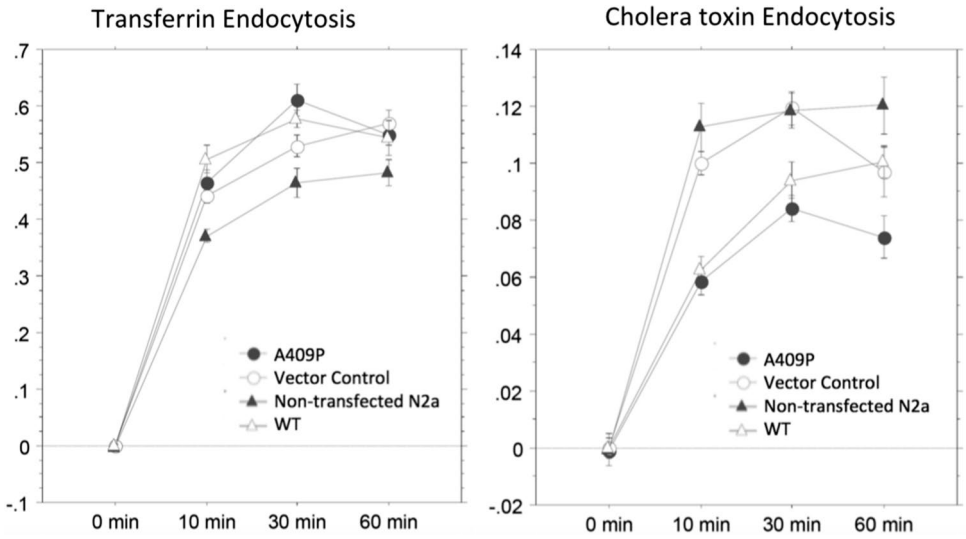

Fig. 5 Quantification of endocytosis of transferrin and cholera toxin subunit B endocytosis. Two replicates/wells were labeled for each transfection group and each time point. For each replicate, eight full-field images were acquired for quantification using a grid-guided systematic random sampling technique. The endocytosis index for each image was calculated as the ratio of the corrected transferrin (TF) or CTB intensities versus those of the DAPI intensity, with the denominator used to correct for different cell densities. Differences between transfection groups were evaluated by Fisher's PLSD post hoc test following ANOVA. Left showed that both WT and A409P transfected N2a cells demonstrated greater TF endocytosis than non-transfected and vector control groups. This effect peaked at 30 min (group effect $F_{(3,60)} = 7.84$, $p = 0.0002$). Right showed that CTB endocytosis was reduced in WT and A409P transfected groups at both 10 and 30 min. However, A409P cells showed persistently lower CTB intensity at 60 min, while WT-transfected cells were similar to the empty control groups. The difference between A409P and WT groups was significant at 60 min ($t = 2.29$, $p = 0.026$)

PPI networks provide molecular evidence for further understanding NHE9's functions and potential mechanisms relevant to ADHD

NHE9 is a pH-regulator for endosomes, and mutations in SLC9A9 alter the endosome pH level and change the trafficking of proteins that depend on this pathway (Kondapalli et al. 2013). However, the molecular mechanisms regulating this function are unknown. The identification of many endosomal vesicle trafficking proteins such as small GTPases, cargo transporters and receptors, and intracellular chaperones supports the role of NHE9 in endocytic protein trafficking. In our work, both the clathrin- and caveolae-mediated endocytosis pathways were significantly enriched for both WT and AP PPIs. Our observation that transferrin endocytosis, an indicator of the clathrin-mediated pathways, was similarly up-regulated in WT and AP transfected cells, was consistent with the pathway enrichment result and previous report (Kondapalli et al. 2013). However, the A409P mutation seemed to preferentially affect the caveolae-mediated endocytosis pathways based on our enrichment results. Caveolae are cholesterol- and sphingolipid-rich, flask-shaped invaginations of the plasma membrane. Caveolae-mediated endocytosis maintains membrane lipid composition and acts as a signaling system. We identified one of the major components of caveolae, flotillin-1(FLOT1) precipitated with the WT NHE9 and an increased precipitation with the A409P mutant protein. This is of particular interest to ADHD because FLOT1 interacts with dopamine transporter (DAT) and is essential for PKC-regulated DAT endocytosis (Sager and Torres 2011; Cremona et al. 2011). Furthermore, our CTB endocytosis assay provided evidence to suggest that the caveolae-mediated endocytosis was preferentially more inhibited by the ADHD-linked A409P mutation. However, CTB can also internalize via other pathways than the caveolae-mediated pathway (Chinnapen et al. 2007). Thus, additional work will be needed to clarify the relationship of NHE9, FLOT1 and caveolae-mediated endocytosis and their roles in ADHD.

Roles of NHE9 PPIs in ASDs

The lack of protein expression of the R423X variant suggests loss of NHE9 function in ASDs. Indeed, two independently developed knockout mice lines both showed autism-like phenotypes (Yang et al. 2016; Ullman et al. 2018). Jacunski (2015) reported that the R423X variant failed to express detectable protein and thus was not studied further. When we examined the overlap of the whole NHE9 network with the SFARI protein interaction network (PIN) for autism, we found that > 90% of NHE9 PPIs were present in the SFARI PIN, a phenomenon similarly observed with other well-known ASD genes, but not with our negative controls (bone marrow density genes). We do not know if the lack

of detectable protein was due to nonsense-mediated mRNA decay or unstable protein degradation, or both.

Notably, MAP2K2, a significantly decreased PPI by ADHD variant A409P, has been linked to cardio-facio-cutaneous syndrome (Karaer et al. 2015; Nowaczyk et al. 2014), one of a family of disorders known as RASopathies that often show autism traits (Adviento et al. 2014). MAP2K2 is a dual specificity protein kinase that belongs to the MAP kinase family (Zheng and Guan 1993a). MAP2K2 phosphorylates and activates MAPK1/ERK2 and MAPK2/ERK3, which subsequently activate MAP kinase-interacting kinases (Mnk1 and Mnk2) (Zheng and Guan 1993b). Interestingly, Mnks are known for phosphorylating EIF4E, an ASD risk gene that was also detected in both WT and AP IP eluates. Phosphorylation of EIF4E by Mnks promotes the dissociation of EIF4E from the FMRP-CYFIP1 complex and the initiation of cap-dependent translation (Beggs et al. 2015; Naegele and Morley 2004; Raught and Gingras 1999), a molecular process disrupted in fragile × mental retardation syndrome (Kremer et al. 1991). Our finding of interaction between NHE9, MAP2K2 and EIF4E may suggest a potential mechanism shared between some ASD and ADHD cases.

Other functions implicated for SLC9A9

Pathway analysis of PPIs suggested putative novel functions for NHE9, such as oxidative stress and mitochondrial dysfunction (Supplementary file 3), both of which have been implicated in ADHD (Joseph et al. 2015) and ASDs (Smaga et al. 2015). Oxidative stress and mitochondrial dysfunction are also associated with inflammatory demyelination in multiple sclerosis (MS) (Mahad et al. 2008), and a pharmacogenetic GWAS found that SLC9A9 was significantly associated with MS disease activity (Esposito et al. 2015), supporting the potential roles of SLC9A9 in these novel functions. Indeed, proteins in NHE family can often interact with many proteins and participate a variety of cellular functions. For example, NHE1 was involved in cellular signaling in response to calcium (Bertrand et al. 1994) and serum (Lehoux et al. 2001), cell survival (Schelling and Abu Jawdeh 2008), oxidative stress (Prasad et al. 2013), dopamine transmission (Rocha et al. 2008), nociception (Castaneda-Corral et al. 2011) and immune responses (De Vito 2006). Proteins and pathways identified from our study suggest that NHE9 may also participate in a variety of cellular functions.

We acknowledge that our methods could identify false positive interactions, such as those that do not happen in vivo. Interactions that we identified will need to be verified using other methods and preferentially verified in situ in the cell. However, it is possible for the intracellular C-terminal of NHE9 to interact with membrane proteins from other organelles when in close proximity and that, subsequently, these interactors can recruit more proteins from those organelles. One example is the endoplasmic reticulum (ER), which can wrap around closely with endosomes (Friedman et al. 2013). Indeed, we identified many ER proteins in the MS results such as several signal peptidase complex (SEC) subunits and several types of signal sequence receptors (SSR).

Our findings suggest a potential role of NHE9 as a local multifunctional signaling scaffold and supported the hypothesis that the endosome functions as a signaling unit (Zhang-James et al. 2012; Dobrowolski and De Robertis 2011), highlighting the potential of targeting the endosome in pharmacological interventions (Palfy et al. 2012).

Rare variants, common mechanisms and potential drug targets

One value of our study resides in testing the paradoxical hypothesis that studies of rare, functional genetic variation can lead to understanding of common mechanisms underlying diseases that have a multifactorial genetic etiology. From a theoretical perspective, it seems reasonable to hypothesize that a common disease-relevant biological pathway implicated by a rare variant could also be degraded by common variants or by environmental risk factors. More importantly, novel pathways and druggable targets discovered from studies of rare variants can lead to treatments that are relevant to patients who do not carry the rare variant. For example, rare variants of PCSK9 cause a rare autosomal dominant familial hypercholesterolemia. Drugs that inhibit PCSK9 are viable treatments for common forms of hypercholesterolemia (Urban et al. 2013; Hooper and Burnett 2013). Canakinumab is a human monoclonal antibody used to treat cryopyrin-associated periodic syndrome, a rare autoinflammatory syndrome caused by mutations in *NLRP3* (Verma et al. 2010). Subsequently, canakinumab was approved for use in common inflammatory syndromes (Onuora 2012; Schlesinger 2012; Alten et al. 2011). Consistent with this idea, our network, derived from rare ASD- and ADHD-risk variants, significantly overlapped with the SFARI PPI network derived from other common and rare risk variants for ASDs, and contained shared functional pathways that may underlie both ADHD and ASDs. Our findings support the possibility that repurposing existing drugs to target the NHE9 network might be useful for treating ADHD (Faraone and Zhang-James 2013) and autism (Lemonnier et al. 2012). It is promising that we found several proteins in the NHE9 network, which were targets of existing drugs currently used for other disorders. Furthermore, many key players of the network could be potentially targeted, such as the mutant altered PPIs and the network hubs. Much work is needed in the future to better understand those targets, and their roles in ADHD and ASDs.

A quantitative proteomic pipeline for evaluation of disease-associated variants: advantages and limitations

Our study provides proof-of-principle for using quantitative MS and co-IP to characterize functional implications of disease-associated variants at the protein level. Our approach can be scaled up to many genes and variants simultaneously and can shed light on both normal gene functioning and the effects of mutations on the disease-relevant interactome. Such work can add valuable insights to the existing and expanding literature of disease-relevant functional protein networks (Corominas et al. 2014; Sakai et al. 2011).

Due to the amount of protein required for IP and MS, and to ensure the antibody used in IP is optimized and not influenced by individual proteins and different mutations, tagged-protein expression in cell lines are the methods of choice at the present. There are several limitations to this approach. First, cell lines may not express neuron-specific proteins such as neurotransmitter receptors and transporters. Future validation studies using neuronal tissue are warranted. Nevertheless, we found that many of our top enriched pathways, such as endocytosis, intracellular signaling cascade and mTOR signaling, were also significantly enriched in gene co-expression networks of SLC9A9 constructed using brain-based RNA-seq data downloaded from BrainSpan (Patak et al. 2017). Furthermore, genes coding proteins from our PPI lists shared significant overlap with genes comprising the co-expression networks of SLC9A9 in several important brain regions including amygdala and frontal cortex (Patak et al. 2017). This suggests that our proteomic findings using the HEK293 cells can identify meaningful functional networks that are important for relevant brain regions. However, we do need to be aware of missed interactions (false negatives) due to no or low expression of target proteins in the cell line. There are several other reasons that we might have false negative findings. For example, transient interactions may not be successfully pulled down and will be missed. Non-specific binding during IP may require more stringent washes or more replicates to ensure that real interactions are not lost due to the noise in the statistical test. Finally, there could be false positive identifications, such as those interactions that do not happen in vivo. Verification of these interactions using different methods and preferentially functional assays in situ in the cell will be needed.

In summary, we used a quantitative proteomic approach to describe NHE9's PPI network and to evaluate the effects of coding variants. These PPI networks confirm the known roles of NHE9 in endosomal pathways and suggest novel functions of the protein. Furthermore, our study identified proteins and pathways affected by disease-relevant coding variants and provided novel hypotheses about the molecular mechanisms associated with ADHD and ASD. Given the availability of 10- and 11-plex TMT reagents, and possibly higher numbers of plexes in the future, our study has demonstrated the feasibility of a parallel and scalable high-throughput platform to characterize many disease-associated genetic variants on functional networks and their potential for drug development.

Note The mass spectrometry proteomics data have been deposited to the ProteomeXchange Consortium via the PRIDE partner repository with the dataset identifier PXD003310.

Acknowledgements We thank Dr. Hanno Steen for helpful advice on proteomics and comments on the manuscript. This work was supported by Stiftelsen Kristian Gerhard Jebsen (SKGJ-MED-002 to Haavik), NIH Grant 5R01MH066877 (Stephen V Faraone, PI) and a NARSAD Young Investigator Award to Yanli Zhang-James. Dr. Faraone is supported by the K. G. Jebsen Centre for Research on Neuropsychiatric Disorders, University of Bergen, Bergen, Norway, the European Union's Seventh Framework Programme for research, technological development and demonstration under Grant Agreement No 602805, the European Union's Horizon 2020 research and innovation programme under Grant Agreement No 667302 and NIMH Grant 5R01MH101519.

Compliance with ethical standards

Conflict of interest Yanli Zhang-James, Frode S. Berven, Olav Mjaavatten, Marc Vaudel and Hanno Steen declare no conflict of interest. During the past three years, Jan Haavik has received speaker fees from Lilly, Novartis, Shire, Medice, HB Pharma and Janssen-Cilag. In the past year, Dr. Faraone received income, travel expenses and/or research support from and/or has been on an Advisory Board for Pfizer, Ironshore, Shire, Akili Interactive Labs, CogCubed, Alcobra, VAYA Pharma, Neurovance, Impax, NeuroLifeSciences and research support from the National Institutes of Health (NIH). With his institution, he has US patent US20130217707 A1 for the use of sodium-hydrogen exchange inhibitors in the treatment of ADHD. In previous years, he received consulting fees or was on Advisory Boards or participated in continuing medical education programs sponsored by: Shire, Alcobra, Otsuka, McNeil, Janssen, Novartis, Pfizer and Eli Lilly. Dr. Faraone receives royalties from books published by Guilford Press: Straight Talk about Your Child's Mental Health, Oxford University Press: Schizophrenia: The Facts and Elsevier, ADHD: Non-Pharmacologic Treatments.

References

Aasebo E, Opsahl JA, Bjorlykke Y, Myhr KM, Kroksveen AC, Berven FS (2014) Effects of blood contamination and the rostro-caudal gradient on the human cerebrospinal fluid proteome. PLoS ONE 9:e90429

Adviento B, Corbin IL, Widjaja F, Desachy G, Enrique N, Rosser T, Risi S, Marco EJ, Hendren RL, Bearden CE, Rauen KA, Weiss LA (2014) Autism traits in the RASopathies. J Med Genet 51:10–20

Alten R, Gomez-Reino J, Durez P, Beaulieu A, Sebba A, Krammer G, Preiss R, Arulmani U, Widmer A, Gitton X, Kellner H (2011) Efficacy and safety of the human anti-IL-1beta monoclonal antibody canakinumab in rheumatoid arthritis: results of a 12-week, Phase II, dose-finding study. BMC Musculoskelet Disord 12:153

Antshel KM, Zhang-James Y, Faraone SV (2013) The comorbidity of ADHD and autism spectrum disorder. Expert Rev Neurother 13:1117–1128

Assenov Y, Ramirez F, Schelhorn SE, Lengauer T, Albrecht M (2008) Computing topological parameters of biological networks. Bioinformatics 24:282–284

Beggs JE, Tian S, Jones GG, Xie J, Iadevaia V, Jenei V, Thomas G, Proud CG (2015) The MAP kinase-interacting kinases regulate cell migration, vimentin expression and eIF4E/CYFIP1 binding. Biochem J 467:63–76

Ben-David E, Shifman S (2012) Networks of neuronal genes affected by common and rare variants in autism spectrum disorders. PLoS Genet 8:e1002556

Bertrand B, Wakabayashi S, Ikeda T, Pouyssegur J, Shigekawa M (1994) The Na^+/H^+ exchanger isoform 1 (NHE1) is a novel member of the calmodulin-binding proteins. Identification and characterization of calmodulin-binding sites. J Biol Chem 269:13703–13709

Biederman J, Monuteaux MC, Faraone SV, Mick E (2009) Parsing the associations between prenatal exposure to nicotine and offspring psychopathology in a nonreferred sample. J Adolesc Health 45:142–148

Brookes K, Xu X, Chen W, Zhou K, Neale B, Lowe N, Anney R, Franke B, Gill M, Ebstein R, Buitelaar J, Sham P, Campbell D, Knight J, Andreou P, Altink M, Arnold R, Boer F, Buschgens C, Butler L, Christiansen H, Feldman L, Fleischman K, Fliers E, Howe-Forbes R, Goldfarb A, Heise A, Gabriels I, Korn-Lubetzki I, Johansson L, Marco R, Medad S, Minderaa R, Mulas F, Muller U, Mulligan A, Rabin K, Rommelse N, Sethna V, Sorohan J, Uebel H, Psychogiou L, Weeks A, Barrett R, Craig I, Banaschewski T, Sonuga-Barke E, Eisenberg J, Kuntsi J, Manor I, McGuffin P, Miranda A, Oades RD, Plomin R, Roeyers H, Rothenberger A, Sergeant J, Steinhausen HC, Taylor E, Thompson M, Faraone SV, Asherson P (2006) The analysis of 51 genes in DSM-IV combined type attention deficit hyperactivity disorder: association signals in DRD4, DAT1 and 16 other genes. Mol Psychiatry 11:934–953

Bullis BL, Li X, Singh DN, Berthiaume LG, Fliegel L (2002) Properties of the Na^+/H^+ exchanger protein. Detergent-resistant aggregation and membrane microdistribution. Eur J Biochem 269:4887–4895

Butland SL, Sanders SS, Schmidt ME, Riechers SP, Lin DT, Martin DD, Vaid K, Graham RK, Singaraja RR, Wanker EE, Conibear E, Hayden MR (2014) The palmitoyl acyltransferase HIP14 shares a high proportion of interactors with huntingtin: implications for a role in the pathogenesis of Huntington's disease. Hum Mol Genet 23:4142–4160

Castaneda-Corral G, Rocha-Gonzalez HI, Godinez-Chaparro B, Jimenez-Andrade JM, Granados-Soto V (2011) Role of the spinal Na^+/H^+ exchanger in formalin-induced nociception. Neurosci Lett 501:4–9

Chen J, Wen J, Zheng Y, Yang H, Luo K, Liu Q, Hu R, Tan Z, Huang Q, Fu J (2015) Prognostic significance of SLC9A9 in patients with resectable esophageal squamous cell carcinoma. Tumour Biol 36:6797–6803

Chinnapen DJ, Chinnapen H, Saslowsky D, Lencer WI (2007) Rafting with cholera toxin: endocytosis and trafficking from plasma membrane to ER. FEMS Microbiol Lett 266:129–137

Corominas R, Yang X, Lin GN, Kang S, Shen Y, Ghamsari L, Broly M, Rodriguez M, Tam S, Trigg SA, Fan C, Yi S, Tasan M, Lemmens I, Kuang X, Zhao N, Malhotra D, Michaelson JJ, Vacic V, Calderwood MA, Roth FP, Tavernier J, Horvath S, Salehi-Ashtiani K, Korkin D, Sebat J, Hill DE, Hao T, Vidal M, Iakoucheva LM (2014) Protein interaction network of alternatively spliced isoforms from brain links genetic risk factors for autism. Nat Commun 5:3650

Cremona ML, Matthies HJ, Pau K, Bowton E, Speed N, Lute BJ, Anderson M, Sen N, Robertson SD, Vaughan RA, Rothman JE, Galli A, Javitch JA, Yamamoto A (2011) Flotillin-1 is essential for PKC-triggered endocytosis and membrane microdomain localization of DAT. Nat Neurosci 14:469–477

Daakour S, Hajingabo LJ, Kerselidou D, Devresse A, Kettmann R, Simonis N, Dequiedt F, Twizere JC (2016) Systematic interactome mapping of acute lymphoblastic leukemia cancer gene products reveals EXT-1 tumor suppressor as a Notch1 and FBWX7 common interactor. BMC Cancer 16:335

Daniels GM, Amara SG (1999) Regulated trafficking of the human dopamine transporter. Clathrin-mediated internalization and lysosomal degradation in response to phorbol esters. J Biol Chem 274:35794–35801

de Silva MG, Elliott K, Dahl HH, Fitzpatrick E, Wilcox S, Delatycki M, Williamson R, Efron D, Lynch M, Forrest S (2003) Disruption of a novel member of a sodium/hydrogen exchanger family and DOCK3 is associated with an attention deficit hyperactivity disorder-like phenotype. J Med Genet 40:733–740

De Vito P (2006) The sodium/hydrogen exchanger: a possible mediator of immunity. Cell Immunol 240:69–85

Demontis D, Walters RK, Martin J, Mattheisen M, Als TD, Agerbo E, Belliveau R, Bybjerg-Grauholm J, Bækved-Hansen M, Cerrato F, Chambert K, Churchhouse C, Dumont A, Eriksson N, Gandal M, Goldstein J, Grove J, Hansen CS, Hauberg M, Hollegaard M, Howrigan DP, Huang H, Maller J, Martin AR, Moran J, Pallesen J, Palmer DS, Pedersen CB, Pedersen MG, Poterba T, Poulsen JB, Ripke S, Robinson EB, Satterstrom FK, Stevens C, Turley P, Won H, Andreassen OA, Burton C, Boomsma D, Cormand B, Dalsgaard S, Franke B, Gelernter J, Geschwind D, Hakonarson H, Haavik J, Kranzler H, Kuntsi J, Langley K, Lesch K-P, Middeldorp C, Reif A, Rohde LA, Roussos P, Schachar R, Sklar P, Sonuga-Barke E, Sullivan PF, Thapar A, Tung J, Waldman I, Nordentoft M, Hougaard DM, Werge T, Mors O, Mortensen PB, Daly MJ, Faraone SV, Børglum AD, Neale BM (2017) Discovery of the first genome-wide significant risk loci for ADHD (submitted for publication)

Dobrowolski R, De Robertis EM (2011) Endocytic control of growth factor signalling: multivesicular bodies as signalling organelles. Nat Rev Mol Cell Biol 13:53–60

Esposito F, Sorosina M, Ottoboni L, Lim ET, Replogle JM, Raj T, Brambilla P, Liberatore G, Guaschino C, Romeo M, Pertel T, Stankiewicz JM, Martinelli V, Rodegher M, Weiner HL, Brassat D, Benoist C, Patsopoulos NA, Comi G, Elyaman W, Martinelli Boneschi F, De Jager PL (2015) A pharmacogenetic study implicates SLC9a9 in multiple sclerosis disease activity. Ann Neurol 78:115–127

Esposito MR, Binatti A, Pantile M, Coppe A, Mazzocco K, Longo L, Capasso M, Lasorsa VA, Luksch R, Bortoluzzi S, Tonini GP (2018) Somatic mutations in specific and connected subpathways are associated with short neuroblastoma patients' survival and indicate proteins targetable at onset of disease. Int J Cancer 143:2525–2536

Faraone SV, Mick E (2010) Molecular genetics of attention deficit hyperactivity disorder. Psychiatr Clin North Am 33:159–180

Faraone SV, Zhang-James Y (2013) Can sodium/hydrogen exchange inhibitors be repositioned for treating attention deficit hyperactivity disorder? An in silico approach. Am J Med Genet B Neuropsychiatr Genet 162B:711–717

Friedman JR, Dibenedetto JR, West M, Rowland AA, Voeltz GK (2013) Endoplasmic reticulum-endosome contact increases as endosomes traffic and mature. Mol Biol Cell 24:1030–1040

Guldbrandsen A, Vethe H, Farag Y, Oveland E, Garberg H, Berle M, Myhr KM, Opsahl JA, Barsnes H, Berven FS (2014) In-depth characterization of the cerebrospinal fluid (CSF) proteome

displayed through the CSF proteome resource (CSF-PR). Mol Cell Proteomics 13:3152–3163

Henningsson S, Jonsson L, Ljunggren E, Westberg L, Gillberg C, Rastam M, Anckarsater H, Nygren G, Landen M, Thuresson K, Betancur C, Leboyer M, Gillberg C, Eriksson E, Melke J (2009) Possible association between the androgen receptor gene and autism spectrum disorder. Psychoneuroendocrinology 34:752–761

Hirling H (2009) Endosomal trafficking of AMPA-type glutamate receptors. Neuroscience 158:36–44

Hisamitsu T, Ben Ammar Y, Nakamura TY, Wakabayashi S (2006) Dimerization is crucial for the function of the Na^+/H^+ exchanger NHE1. Biochemistry 45:13346–13355

Hooper AJ, Burnett JR (2013) Anti-PCSK9 therapies for the treatment of hypercholesterolemia. Expert Opin Biol Ther 13:429–435

Hultman CM, Torrang A, Tuvblad C, Cnattingius S, Larsson JO, Lichtenstein P (2007) Birth weight and attention-deficit/hyperactivity symptoms in childhood and early adolescence: a prospective swedish twin study. J Am Acad Child Adolesc Psychiatry 46:370–377

Jacunski M (2015) The role of NHE9 in vesicular trafficking and pH regulation. McGill University, Montreal

Joseph N, Zhang-James Y, Perl A, Faraone SV (2015) Oxidative stress and ADHD: a meta-analysis. J Atten Disord 19:915–924

Karaer K, Lissewski C, Zenker M (2015) Familial cardiofaciocutaneous syndrome in a father and a son with a novel MEK2 mutation. Am J Med Genet A 167A:385–388

Kondapalli KC, Hack A, Schushan M, Landau M, Ben-Tal N, Rao R (2013) Functional evaluation of autism-associated mutations in NHE9. Nat Commun 4:2510

Kremer EJ, Pritchard M, Lynch M, Yu S, Holman K, Baker E, Warren ST, Schlessinger D, Sutherland GR, Richards RI (1991) Mapping of DNA instability at the fragile X to a trinucleotide repeat sequence p(CCG)n. Science 252:1711–1714

Lanz TA, Guilmette E, Gosink MM, Fischer JE, Fitzgerald LW, Stephenson DT, Pletcher MT (2013) Transcriptomic analysis of genetically defined autism candidate genes reveals common mechanisms of action. Mol Autism 4:45

Lasky-Su J, Anney RJ, Neale BM, Franke B, Zhou K, Maller JB, Vasquez AA, Chen W, Asherson P, Buitelaar J, Banaschewski T, Ebstein R, Gill M, Miranda A, Mulas F, Oades RD, Roeyers H, Rothenberger A, Sergeant J, Sonuga-Barke E, Steinhausen HC, Taylor E, Daly M, Laird N, Lange C, Faraone SV (2008a) Genome-wide association scan of the time to onset of attention deficit hyperactivity disorder. Am J Med Genet B Neuropsychiatr Genet 147B:1355–1358

Lasky-Su J, Neale BM, Franke B, Anney RJ, Zhou K, Maller JB, Vasquez AA, Chen W, Asherson P, Buitelaar J, Banaschewski T, Ebstein R, Gill M, Miranda A, Mulas F, Oades RD, Roeyers H, Rothenberger A, Sergeant J, Sonuga-Barke E, Steinhausen HC, Taylor E, Daly M, Laird N, Lange C, Faraone SV (2008b) Genome-wide association scan of quantitative traits for attention deficit hyperactivity disorder identifies novel associations and confirms candidate gene associations. Am J Med Genet B Neuropsychiatr Genet 147B:1345–1354

Lee SH, Ripke S, Neale BM, Faraone SV, Purcell SM, Perlis RH, Mowry BJ, Thapar A, Goddard ME, Witte JS, Absher D, Agartz I, Akil H, Amin F, Andreassen OA, Anjorin A, Anney R, Anttila V, Arking DE, Asherson P, Azevedo MH, Backlund L, Badner JA, Bailey AJ, Banaschewski T, Barchas JD, Barnes MR, Barrett TB, Bass N, Battaglia A, Bauer M, Bayes M, Bellivier F, Bergen SE, Berrettini W, Betancur C, Bettecken T, Biederman J, Binder EB, Black DW, Blackwood DH, Bloss CS, Boehnke M, Boomsma DI, Breen G, Breuer R, Bruggeman R, Cormican P, Buccola NG, Buitelaar JK, Bunney WE, Buxbaum JD, Byerley WF, Byrne EM, Caesar S, Cahn W, Cantor RM, Casas M, Chakravarti A, Chambert K, Choudhury K, Cichon S, Cloninger CR, Collier DA, Cook EH, Coon H, Cormand B, Corvin A, Coryell WH, Craig DW, Craig IW, Crosbie J, Cuccaro ML, Curtis D, Czamara D, Datta S, Dawson G, Day R, De Geus EJ, Degenhardt F, Djurovic S, Donohoe GJ, Doyle AE, Duan J, Dudbridge F, Duketis E, Ebstein RP, Edenberg HJ, Elia J, Ennis S, Etain B, Fanous A, Farmer AE, Ferrier IN, Flickinger M, Fombonne E, Foroud T, Frank J, Franke B, Fraser C, Freedman R, Freimer NB, Freitag CM, Friedl M, Frisen L, Gallagher L, Gejman PV, Georgieva L, Gershon ES, Geschwind DH, Giegling I, Gill M, Gordon SD, Gordon-Smith K, Green EK, Greenwood TA, Grice DE, Gross M, Grozeva D, Guan W, Gurling H, De Haan L, Haines JL, Hakonarson H, Hallmayer J, Hamilton SP, Hamshere ML, Hansen TF, Hartmann AM, Hautzinger M, Heath AC, Henders AK, Herms S, Hickie IB, Hipolito M, Hoefels S, Holmans PA, Holsboer F, Hoogendijk WJ, Hottenga JJ, Hultman CM, Hus V, Ingason A, Ising M, Jamain S, Jones EG, Jones I, Jones L, Tzeng JY, Kahler AK, Kahn RS, Kandaswamy R, Keller MC, Kennedy JL, Kenny E, Kent L, Kim Y, Kirov GK, Klauck SM, Klei L, Knowles JA, Kohli MA, Koller DL, Konte B, Korszun A, Krabbendam L, Krasucki R, Kuntsi J, Kwan P, Landen M, Langstrom N, Lathrop M, Lawrence J, Lawson WB, Leboyer M, Ledbetter DH, Lee PH, Lencz T, Lesch KP, Levinson DF, Lewis CM, Li J, Lichtenstein P, Lieberman JA, Lin DY, Linszen DH, Liu C, Lohoff FW, Loo SK, Lord C, Lowe JK, Lucae S, MacIntyre DJ, Madden PA, Maestrini E, Magnusson PK, Mahon PB, Maier W, Malhotra AK, Mane SM, Martin CL, Martin NG, Mattheisen M, Matthews K, Mattingsdal M, McCarroll SA, McGhee KA, McGough JJ, McGrath PJ, McGuffin P, McInnis MG, McIntosh A, McKinney R, McLean AW, McMahon FJ, McMahon WM, McQuillin A, Medeiros H, Medland SE, Meier S, Melle I, Meng F, Meyer J, Middeldorp CM, Middleton L, Milanova V, Miranda A, Monaco AP, Montgomery GW, Moran JL, Moreno-De-Luca D, Morken G, Morris DW, Morrow EM, Moskvina V, Muglia P, Muhleisen TW, Muir WJ, Muller-Myhsok B, Murtha M, Myers RM, Myin-Germeys I, Neale MC, Nelson SF, Nievergelt CM, Nikolov I, Nimgaonkar V, Nolen WA, Nothen MM, Nurnberger JI, Nwulia EA, Nyholt DR, O'Dushlaine C, Oades RD, Olincy A, Oliveira G, Olsen L, Ophoff RA, Osby U, Owen MJ, Palotie A, Parr JR, Paterson AD, Pato CN, Pato MT, Penninx BW, Pergadia ML, Pericak-Vance MA, Pickard BS, Pimm J, Piven J, Posthuma D, Potash JB, Poustka F, Propping P, Puri V, Quested DJ, Quinn EM, Ramos-Quiroga JA, Rasmussen HB, Raychaudhuri S, Rehnstrom K, Reif A, Ribases M, Rice JP, Rietschel M, Roeder K, Roeyers H, Rossin L, Rothenberger A, Rouleau G, Ruderfer D, Rujescu D, Sanders AR, Sanders SJ, Santangelo SL, Sergeant JA, Schachar R, Schalling M, Schatzberg AF, Scheftner WA, Schellenberg GD, Scherer SW, Schork NJ, Schulze TG, Schumacher J, Schwarz M, Scolnick E, Scott LJ, Shi J, Shilling PD, Shyn SI, Silverman JM, Slager SL, Smalley SL, Smit JH, Smith EN, Sonuga-Barke EJ, St Clair D, State M, Steffens M, Steinhausen HC, Strauss JS, Strohmaier J, Stroup TS, Sutcliffe JS, Szatmari P, Szelinger S, Thirumalai S, Thompson RC, Todorov AA, Tozzi F, Treutlein J, Uhr M, van den Oord EJ, Van Grootheest G, Van Os J, Vicente AM, Vieland VJ, Vincent JB, Visscher PM, Walsh CA, Wassink TH, Watson SJ, Weissman MM, Werge T, Wienker TF, Wijsman EM, Willemsen G, Williams N, Willsey AJ, Witt SH, Xu W, Young AH, Yu TW, Zammit S, Zandi PP, Zhang P, Zitman FG, Zollner S, Devlin B, Kelsoe JR, Sklar P, Daly MJ, O'Donovan MC, Craddock N, Sullivan PF, Smoller JW, Kendler KS, Wray NR (2013) Genetic relationship between five psychiatric disorders estimated from genome-wide SNPs. Nat Genet 45:984–994

Lehoux S, Abe J, Florian JA, Berk BC (2001) 14-3-3 Binding to Na^+/H^+ exchanger isoform-1 is associated with serum-dependent activation of Na^+/H^+ exchange. J Biol Chem 276:15794–15800

Lemonnier E, Degrez C, Phelep M, Tyzio R, Josse F, Grandgeorge M, Hadjikhani N, Ben-Ari Y (2012) A randomised controlled trial of bumetanide in the treatment of autism in children. Transl Psychiatry 2:e202

Liu G, Zhang F, Hu Y, Jiang Y, Gong Z, Liu S, Chen X, Jiang Q, Hao J (2017) Genetic variants and multiple sclerosis risk gene SLC9A9 expression in distinct human brain regions. Mol Neurobiol 54:6820–6826

Mahad D, Lassmann H, Turnbull D (2008) Review: mitochondria and disease progression in multiple sclerosis. Neuropathol Appl Neurobiol 34:577–589

Mahoney DW, Therneau TM, Heppelmann CJ, Higgins L, Benson LM, Zenka RM, Jagtap P, Nelsestuen GL, Bergen HR, Oberg AL (2011) Relative quantification: characterization of bias, variability and fold changes in mass spectrometry data from iTRAQ-labeled peptides. J Proteome Res 10:4325–4333

Malo ME, Fliegel L (2006) Physiological role and regulation of the Na^+/H^+ exchanger. Can J Physiol Pharmacol 84:1081–1095

Markunas CA, Quinn KS, Collins AL, Garrett ME, Lachiewicz AM, Sommer JL, Morrissey-Kane E, Kollins SH, Anastopoulos AD, Ashley-Koch AE (2010) Genetic variants in SLC9A9 are associated with measures of attention-deficit/hyperactivity disorder symptoms in families. Psychiatr Genet 20:73–81

Martin-Negrier ML, Charron G, Bloch B (2006) Receptor recycling mediates plasma membrane recovery of dopamine D1 receptors in dendrites and axons after agonist-induced endocytosis in primary cultures of striatal neurons. Synapse 60:194–204

Martinussen R, Tannock R (2006) Working memory impairments in children with attention-deficit hyperactivity disorder with and without comorbid language learning disorders. J Clin Exp Neuropsychol 28:1073–1094

Mayle KM, Le AM, Kamei DT (2012) The intracellular trafficking pathway of transferrin. Biochim Biophys Acta 1820:264–281

Melikian HE, Buckley KM (1999) Membrane trafficking regulates the activity of the human dopamine transporter. J Neurosci 19:7699–7710

Monuteaux MC, Spencer TJ, Faraone SV, Wilson AM, Biederman J (2007) A randomized, placebo-controlled clinical trial of bupropion for the prevention of smoking in children and adolescents with attention-deficit/hyperactivity disorder. J Clin Psychiatry 68:1094–1101

Morrow EM, Yoo SY, Flavell SW, Kim TK, Lin Y, Hill RS, Mukaddes NM, Balkhy S, Gascon G, Hashmi A, Al-Saad S, Ware J, Joseph RM, Greenblatt R, Gleason D, Ertelt JA, Apse KA, Bodell A, Partlow JN, Barry B, Yao H, Markianos K, Ferland RJ, Greenberg ME, Walsh CA (2008) Identifying autism loci and genes by tracing recent shared ancestry. Science 321:218–223

Naegele Susanne, Morley Simon J (2004) Molecular cross-talk between MEK1/2 and mTOR signaling during recovery of 293 cells from hypertonic stress. J Biol Chem 279:46023–46034

Nakamura N, Tanaka S, Teko Y, Mitsui K, Kanazawa H (2005) Four Na^+/H^+ exchanger isoforms are distributed to Golgi and post-Golgi compartments and are involved in organelle pH regulation. J Biol Chem 280:1561–1572

Neale BM, Kou Y, Liu L, Ma'ayan A, Samocha KE, Sabo A, Lin CF, Stevens C, Wang LS, Makarov V, Polak P, Yoon S, Maguire J, Crawford EL, Campbell NG, Geller ET, Valladares O, Schafer C, Liu H, Zhao T, Cai G, Lihm J, Dannenfelser R, Jabado O, Peralta Z, Nagaswamy U, Muzny D, Reid JG, Newsham I, Wu Y, Lewis L, Han Y, Voight BF, Lim E, Rossin E, Kirby A, Flannick J, Fromer M, Shakir K, Fennell T, Garimella K, Banks E, Poplin R, Gabriel S, DePristo M, Wimbish JR, Boone BE, Levy SE, Betancur C, Sunyaev S, Boerwinkle E, Buxbaum JD, Cook EH Jr, Devlin B, Gibbs RA, Roeder K, Schellenberg GD, Sutcliffe JS, Daly MJ (2012) Patterns and rates of exonic de novo mutations in autism spectrum disorders. Nature 485:242–245

Ng D, Hu N, Hu Y, Wang C, Giffen C, Tang ZZ, Han XY, Yang HH, Lee MP, Goldstein AM, Taylor PR (2008) Replication of a genome-wide case-control study of esophageal squamous cell carcinoma. Int J Cancer 123:1610–1615

Ngounou Wetie AG, Wormwood K, Thome J, Dudley E, Taurines R, Gerlach M, Woods AG, Darie CC (2014) A pilot proteomic study of protein markers in autism spectrum disorder. Electrophoresis 35:2046–2054

Ngounou Wetie AG, Wormwood KL, Charette L, Ryan JP, Woods AG, Darie CC (2015) Comparative two-dimensional polyacrylamide gel electrophoresis of the salivary proteome of children with autism spectrum disorder. J Cell Mol Med 19:2664–2678

Nowaczyk MJ, Thompson BA, Zeesman S, Moog U, Sanchez-Lara PA, Magoulas PL, Falk RE, Hoover-Fong JE, Batista DA, Amudhavalli SM, White SM, Graham GE, Rauen KA (2014) Deletion of MAP2K2/MEK2: a novel mechanism for a RASopathy? Clin Genet 85:138–146

Oberg AL, Mahoney DW (2012) Statistical methods for quantitative mass spectrometry proteomic experiments with labeling. BMC Bioinform 13(Suppl 16):S7

Oberg AL, Vitek O (2009) Statistical design of quantitative mass spectrometry-based proteomic experiments. J Proteome Res 8:2144–2156

Ohgaki R, Fukura N, Matsushita M, Mitsui K, Kanazawa H (2008) Cell surface levels of organellar Na^+/H^+ exchanger isoform 6 are regulated by interaction with RACK1. J Biol Chem 283:4417–4429

Onuora S (2012) Crystal arthritis: canakinumab relieves gout flares when treatment options are limited. Nat Rev Rheumatol 8:369

O'Roak BJ, Deriziotis P, Lee C, Vives L, Schwartz JJ, Girirajan S, Karakoc E, Mackenzie AP, Ng SB, Baker C, Rieder MJ, Nickerson DA, Bernier R, Fisher SE, Shendure J, Eichler EE (2011) Exome sequencing in sporadic autism spectrum disorders identifies severe de novo mutations. Nat Genet 43:585–589

O'Roak BJ, Vives L, Fu W, Egertson JD, Stanaway IB, Phelps IG, Carvill G, Kumar A, Lee C, Ankenman K, Munson J, Hiatt JB, Turner EH, Levy R, O'Day DR, Krumm N, Coe BP, Martin BK, Borenstein E, Nickerson DA, Mefford HC, Doherty D, Akey JM, Bernier R, Eichler EE, Shendure J (2012) Multiplex targeted sequencing identifies recurrently mutated genes in autism spectrum disorders. Science 338:1619–1622

Palfy M, Remenyi A, Korcsmaros T (2012) Endosomal crosstalk: meeting points for signaling pathways. Trends Cell Biol 22:447–456

Park M, Penick EC, Edwards JG, Kauer JA, Ehlers MD (2004) Recycling endosomes supply AMPA receptors for LTP. Science 305:1972–1975

Park M, Salgado JM, Ostroff L, Helton TD, Robinson CG, Harris KM, Ehlers MD (2006) Plasticity-induced growth of dendritic spines by exocytic trafficking from recycling endosomes. Neuron 52:817–830

Patak J, Zhang-James Y, Faraone SV (2016) Endosomal system genetics and autism spectrum disorders: a literature review. Neurosci Biobehav Rev 65:95–112

Patak J, Hess JL, Zhang-James Y, Glatt SJ, Faraone SV (2017) SLC9A9 Co-expression modules in autism-associated brain regions. Autism Res 10:414–429

Pivac N, Knezevic A, Gornik O, Pucic M, Igl W, Peeters H, Crepel A, Steyaert J, Novokmet M, Redzic I, Nikolac M, Hercigonja VN, Curkovic KD, Curkovic M, Nedic G, Muck-Seler D, Borovecki F, Rudan I, Lauc G (2011) Human plasma glycome in attention-deficit hyperactivity disorder and autism spectrum disorders. Mol Cell Proteomics 10(M110):004200

Poelmans G, Pauls DL, Buitelaar JK, Franke B (2011) Integrated genome-wide association study findings: identification of a neurodevelopmental network for attention deficit hyperactivity disorder. Am J Psychiatry 168:365–377

Prasad V, Lorenz JN, Miller ML, Vairamani K, Nieman ML, Wang Y, Shull GE (2013) Loss of NHE1 activity leads to reduced oxidative stress in heart and mitigates high-fat diet-induced myocardial stress. J Mol Cell Cardiol 65:33–42

Ralston SH, de Crombrugghe B (2006) Genetic regulation of bone mass and susceptibility to osteoporosis. Genes Dev 20:2492–2506

Raught B, Gingras AC (1999) eIF4E activity is regulated at multiple levels. Int J Biochem Cell Biol 31:43–57

Ritchie ME, Phipson B, Wu D, Hu Y, Law CW, Shi W, Smyth GK (2015) limma powers differential expression analyses for RNA-sequencing and microarray studies. Nucleic Acids Res 43:e47

Rocha MA, Crockett DP, Wong LY, Richardson JR, Sonsalla PK (2008) Na(+)/H(+) exchanger inhibition modifies dopamine neurotransmission during normal and metabolic stress conditions. J Neurochem 106:231–243

Sager JJ, Torres GE (2011) Proteins interacting with monoamine transporters: current state and future challenges. Biochemistry 50:7295–7310

Sagvolden T, Dasbanerjee T, Zhang-James Y, Middleton F, Faraone S (2008) Behavioral and genetic evidence for a novel animal model of Attention-Deficit/Hyperactivity Disorder Predominantly Inattentive Subtype. Behav Brain Funct 4:56

Sakai Y, Shaw CA, Dawson BC, Dugas DV, Al-Mohtaseb Z, Hill DE, Zoghbi HY (2011) Protein interactome reveals converging molecular pathways among autism disorders. Sci Transl Med 3:86ra49

Sanders SJ, Murtha MT, Gupta AR, Murdoch JD, Raubeson MJ, Willsey AJ, Ercan-Sencicek AG, DiLullo NM, Parikshak NN, Stein JL, Walker MF, Ober GT, Teran NA, Song Y, El-Fishawy P, Murtha RC, Choi M, Overton JD, Bjornson RD, Carriero NJ, Meyer KA, Bilguvar K, Mane SM, Sestan N, Lifton RP, Gunel M, Roeder K, Geschwind DH, Devlin B, State MW (2012) De novo mutations revealed by whole-exome sequencing are strongly associated with autism. Nature 485:237–241

Schelling JR, Abu Jawdeh BG (2008) Regulation of cell survival by Na^+/H^+ exchanger-1. Am J Physiol Renal Physiol 295:F625–F632

Schlesinger N (2012) Canakinumab in gout. Expert Opin Biol Ther 12:1265–1275

Schneider CA, Rasband WS, Eliceiri KW (2012) NIH Image to ImageJ: 25 years of image analysis. Nat Methods 9:671–675

Shannon P, Markiel A, Ozier O, Baliga NS, Wang JT, Ramage D, Amin N, Schwikowski B, Ideker T (2003) Cytoscape: a software environment for integrated models of biomolecular interaction networks. Genome Res 13:2498–2504

Smaga I, Niedzielska E, Gawlik M, Moniczewski A, Krzek J, Przegalinski E, Pera J, Filip M (2015) Oxidative stress as an etiological factor and a potential treatment target of psychiatric disorders. Part 2. Depression, anxiety, schizophrenia and autism. Pharmacol Rep 67:569–580

Smyth GK, Speed T (2003) Normalization of cDNA microarray data. Methods 31:265–273

Solomon M, Frank MJ, Ragland JD, Smith AC, Niendam TA, Lesh TA, Grayson DS, Beck JS, Matter JC, Carter CS (2015) Feedback-driven trial-by-trial learning in autism spectrum disorders. Am J Psychiatry 172:173–181

Sowerby P, Seal S, Tripp G (2011) Working memory deficits in ADHD: the contribution of age, learning/language difficulties, and task parameters. J Atten Disord 15:461–472

Taurines R, Dudley E, Conner AC, Grassl J, Jans T, Guderian F, Mehler-Wex C, Warnke A, Gerlach M, Thome J (2010) Serum protein profiling and proteomics in autistic spectrum disorder using magnetic bead-assisted mass spectrometry. Eur Arch Psychiatry Clin Neurosci 260:249–255

Turkewitz AP, Amatruda JF, Borhani D, Harrison SC, Schwartz AL (1988) A high yield purification of the human transferrin receptor and properties of its major extracellular fragment. J Biol Chem 263:8318–8325

Uhl GR, Liu QR, Drgon T, Johnson C, Walther D, Rose JE (2007) Molecular genetics of nicotine dependence and abstinence: whole genome association using 520,000 SNPs. BMC Genet 8:10

Ullman JC, Yang J, Sullivan M, Bendor J, Levy J, Pham E, Silm K, Seifikar H, Sohal VS, Nicoll RA, Edwards RH (2018) A mouse model of autism implicates endosome pH in the regulation of presynaptic calcium entry. Nat Commun 9:330

Urban D, Poss J, Bohm M, Laufs U (2013) Targeting the proprotein convertase subtilisin/kexin type 9 for the treatment of dyslipidemia and atherosclerosis. J Am Coll Cardiol 62:1401–1408

Verma D, Eriksson P, Sahdo B, Persson A, Ejdeback M, Sarndahl E, Soderkvist P (2010) Two adult siblings with atypical cryopyrin-associated periodic syndrome due to a novel M299V mutation in NLRP3. Arthritis Rheum 62:2138–2143

Wagle M, Holder J (2014) Exonic deletion of SLC9A9 in autism with epilepsy. Neurology 82:P4.338

Williams NM, Franke B, Mick E, Anney RJ, Freitag CM, Gill M, Thapar A, O'Donovan MC, Owen MJ, Holmans P, Kent L, Middleton F, Zhang-James Y, Liu L, Meyer J, Nguyen TT, Romanos J, Romanos M, Seitz C, Renner TJ, Walitza S, Warnke A, Palmason H, Buitelaar J, Rommelse N, Vasquez AA, Hawi Z, Langley K, Sergeant J, Steinhausen HC, Roeyers H, Biederman J, Zaharieva I, Hakonarson H, Elia J, Lionel AC, Crosbie J, Marshall CR, Schachar R, Scherer SW, Todorov A, Smalley SL, Loo S, Nelson S, Shtir C, Asherson P, Reif A, Lesch KP, Faraone SV (2012) Genome-wide analysis of copy number variants in attention deficit/hyperactivity disorder confirms the role of rare variants and implicates duplications at 15q13.3. Am J Psychiatry 169:195–204

Woods AG, Ngounou Wetie AG, Sokolowska I, Russell S, Ryan JP, Michel TM, Thome J, Darie CC (2013) Mass spectrometry as a tool for studying autism spectrum disorder. J Mol Psychiatry 1:6

Yang L, Neale BM, Liu L, Lee SH, Wray NR, Ji N, Li H, Qian Q, Wang D, Li J, Faraone SV, Wang Y (2013) Polygenic transmission and complex neuro developmental network for attention deficit hyperactivity disorder: genome-wide association study of both common and rare variants. Am J Med Genet B Neuropsychiatr Genet 162:419–430

Yang L, Faraone SV, Zhang-James Y (2016) Autism spectrum disorder traits in Slc9a9 knock-out mice. Am J Med Genet B Neuropsychiatr Genet 171B:363–376

Zafeiriou DI, Ververi A, Dafoulis V, Kalyva E, Vargiami E (2013) Autism spectrum disorders: the quest for genetic syndromes. Am J Med Genet B Neuropsychiatr Genet 162B:327–366

Zayats T, Athanasiu L, Sonderby I, Djurovic S, Westlye LT, Tamnes CK, Fladby T, Aase H, Zeiner P, Reichborn-Kjennerud T, Knappskog PM, Knudsen GP, Andreassen OA, Johansson S, Haavik J (2015) Genome-wide analysis of attention deficit hyperactivity disorder in Norway. PLoS ONE 10:e0122501

Zhang-James Y, DasBanerjee T, Sagvolden T, Middleton FA, Faraone SV (2011) SLC9A9 mutations, gene expression, and protein-protein interactions in rat models of attention-deficit/hyperactivity disorder. Am J Med Genet Part B Neuropsychiatr Genet 156:835–843

Zhang-James Y, Middleton FA, Sagvolden T, Faraone SV (2012) Differential expression of SLC9A9 and interacting molecules in the hippocampus of rat models for attention deficit/hyperactivity disorder. Dev Neurosci 34:218–227

Zhang-James Y, Yang L, Middleton FA, Yang L, Patak J, Faraone SV (2014) Autism-related behavioral phenotypes in an inbred rat substrain. Behav Brain Res 269:103–114

Zheng CF, Guan KL (1993a) Cloning and characterization of two distinct human extracellular signal-regulated kinase activator kinases, MEK1 and MEK2. J Biol Chem 268:11435–11439

Zheng CF, Guan KL (1993b) Properties of MEKs, the kinases that phosphorylate and activate the extracellular signal-regulated kinases. J Biol Chem 268:23933–23939